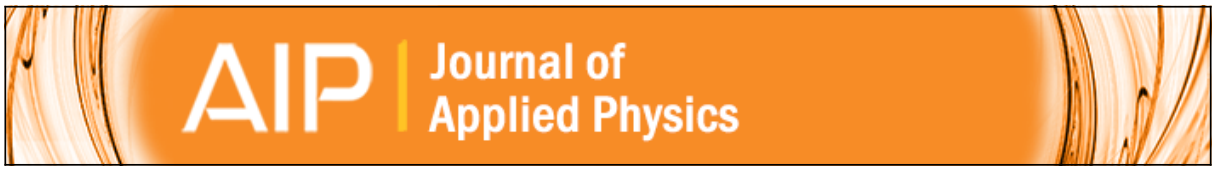

Photoelectron spectra of amorphous Si x H y alloy films: The effect of microstructure on the Si2p level shift

S. R. Das, J. B. Webb, S. C. de Castro, and V. S. Sundaram

Citation: Journal of Applied Physics **60**, 2530 (1986); doi: 10.1063/1.337116

View online: http://dx.doi.org/10.1063/1.337116

View Table of Contents: http://scitation.aip.org/content/aip/journal/jap/60/7?ver=pdfcov

Published by the AIP Publishing

Photoelectron spectra of amorphous Si_xH_y alloy films: The effect of microstructure on the Si-2*p* level shift

S. R. Das and J. B. Webb
National Research Council of Canada, Ottawa, Ontario K1A OR6, Canada

S. C. de Castro and V. S. Sundaram[a)]
Instituto De Fisica, Universidade Estadual De Campinas, Caixa Postal 1170, 13100 Campinas SP, Brazil

(Received 26 March 1986; accepted for publication 30 May 1986)

Depending on the deposition conditions, amorphous Si_xH_y alloy films prepared by planar rf reactive magnetron sputtering exhibit one of three types of microstructure: (i) type A with no discernible microstructural features down to the 20-Å level and with a smooth uniform density; (ii) type B consisting of high-density regions of 50–200-Å lateral dimensions separated by a low-density network; and (iii) a two-level (type C) microstructure consisting of 300–500-Å dimensions columns separated by a pronounced low-density network. The columns, in turn, are composed of 50–200-Å dimension high-density regions interspersed with low-density network. The Si-2*p* level in these alloy films, determined by x-ray photoelectron spectroscopy, is observed to be strongly influenced by the microstructure of the film. A shift in the Si-2*p* level, systematically varying with the hydrogen concentration, is observed in alloy films with type B and type C microstructures. No shift is observed, irrespective of the hydrogen concentration, in alloy films with type A microstructure. The photoelectron spectra are examined in the light of the vibrational spectra of the films as measured by Fourier transform infrared techniques. The dependence of the Si-2*p* level shift on the microstructure and the variation with hydrogen concentration are explained qualitatively in terms of the differences in the silicon–hydrogen bonding in amorphous Si_xH_y films with dissimilar microstructures.

INTRODUCTION

It is well established empirically that alloying of amorphous silicon with hydrogen lowers the density of gap states from about 10^{20} eV^{-1} cm^{-3} for pure amorphous silicon (*a*-Si) to values as low as about 10^{15} eV^{-1} cm^{-3} for alloy (*a*-Si_xH_y) films leading to a material that is electronically, optically, and optoelectronically superior.[1,2] Although the role played by hydrogen in improving the properties of *a*-Si is only partially understood, it is fairly evident from electron-spin resonance measurements that a fraction of the hydrogen atoms serve to saturate dangling bonds (unsatisfied Si bonds) in the amorphous network, thus quenching the spin centers associated with unpaired electrons in the dangling bonds. Since the amorphous network is composed of Si tetrahedra which retain essentially the bond length and bond angle of crystalline silicon, there exists a variety of Si–H bonding configurations involving between 1 and 4 hydrogen atoms attached to a silicon atom, viz., SiH, SiH_2, SiH_3, and $(SiH_2)_n$. Infrared spectroscopy, directed towards measuring the frequencies and intensities of the vibrational modes of the silicon–hydrogen bonds, has provided the bulk of the information on bonding configurations and their dependence on growth conditions.[3–6] More recently, photoelectron spectroscopy investigations, aimed at studying the effect of hydrogenation on the Si-2*p* core level spectra and valence band spectra in amorphous Si_xH_y films, have been reported.[7,8] Ley *et al.*[8,9] have investigated the effect of hydrogenation and fluorination on the Si-2*p* core level spectra in amorphous hydrogenated silicon and amorphous fluorinated silicon samples and have analyzed the spectra in terms of the differences in the relative contributions to the spectra from different bonding (Si–H or Si–F) configurations. However, the authors have not included any supporting infrared data on the samples. Moreover, the effect of the microstructure of the films on the Si-2*p* core level spectra has not been studied, although one would expect to observe changes in the Si-2*p* core level spectra due to differences in the microstructure of the films based on the association of different silicon–hydrogen bonding configurations with specific microstructural features as noted by several workers.[3–5,10,11]

In previous publications [12–16] we have reported on the preparation and properties of amorphous Si_xH_y alloy (*a*-Si_xH_y) films by planar, reactive, rf magnetron sputtering. Hydrogen profiling by a ^{15}N bombardment technique shows that, independent of the microstructure, the hydrogen content (H/host) can be varied up to 50% depending primarily on the hydrogen partial pressure during deposition.[15] However, the microstructure of the film in particular influences the low-temperature hydrogen evolution.[15] The photoconductivity in the *a*-Si_xH_y films is observed to depend sensitively on the microstructure.[16] In particular, the interrelationship between the dark conductivity (σ_{dark}), the photoconductivity (σ_{ph}), the photoconducting gain ($\sigma_{ph}/\sigma_{dark}$), and the optical band gap (E_g) of a film is strongly influenced by the microstructure. Thus films with a particular combination of σ_{dark}, σ_{ph}, $\sigma_{ph}/\sigma_{dark}$, and E_g can only be prepared with a specific microstructure. We suggest that the

[a)] Present address: General Optronics, 2 Olsen Avenue, Edison, NJ 08820.

 0021-8979/86/192530-06$02.40

observed microstructure effects mentioned above can be explained qualitatively on the basis of the differences in the silicon–hydrogen bonding configuration in films with dissimilar microstructures but the same total hydrogen concentration. We have, therefore, investigated by x-ray photoelectron spectroscopy the effect of film microstructure on the Si-2p level in a-Si_xH_y alloy films prepared by rf magnetron sputtering. In this paper we discuss the results of our photoelectron spectroscopy investigations in the light of the infrared data on the vibrational modes in these films.

EXPERIMENT

Amorphous Si_xH_y alloy films were prepared on Corning 7059 glass and single crystal silicon wafers (for Fourier-transform infrared measurements) by planar, reactive, rf magnetron sputtering in a cryo-pumped stainless steel chamber using a 10-cm-diam, polycrystalline, 99.999% pure silicon plate as the cathode. The base pressure was typically 2×10^{-7} Torr. The flow rates and hence, the partial pressures, of the sputtering gas (Ar) and the reactive gas (H_2) were controlled by electronic mass flow controllers to within 0.1 sccm for Ar and 0.001 sccm for H_2. The rf power to the cathode was fed via a feedback circuit to maintain constant target bias. Details of the sputtering system have been published elsewhere.[12] The deposition ranges covered for this study were: rf power 50–500 W, argon partial pressure 1.0–10 mTorr, hydrogen partial pressure 2×10^{-4} mTorr (residual pressure in chamber for no added hydrogen) -1.7 mTorr, and substrate temperature 300–600 K.

X-ray photoelectron spectroscopy (XPS) measurements were performed in a McPherson ESCA-36 spectrometer using Al $K\alpha$ excitation at a base pressure of $\sim1\times10^{-8}$ Torr. The spectrometer was calibrated with respect to the Au-4f7/2 line (i.e., 84.0 eV). Since the a-Si_xH_y samples studied were nonconductive, the binding energies were referenced to the carbon 1s line (i.e., 285.0 eV) from the samples.

Electron diffraction and normal imaging of the microstructure were checked for several samples in a Siemens 101 transmission electron microscope. Details of the sample preparation and microscopy techniques have been reported previously.[14]

Specular transmittance and reflectance data in the frequency range 500–2500 cm^{-1} were obtained on a-Si_xH_y samples prepared on single crystal silicon wafers using a BOMEM Fourier transform infrared (FTIR) spectrometer. The optical constants and hence, the absorption coefficient α, were determined from the reflectance and transmittance data by the method of inverse synthesis described by Dobrowolski *et al.*[17]

The total hydrogen content in the films was measured[15] from nuclear-reaction analysis by bombardment with ^{15}N based on the nuclear reaction $^{15}N + {}^1H \rightarrow {}^{12}C + {}^4He + 4.43\text{-MeV } \gamma$ ray. The temperature dependence of the hydrogen evolution rate was measured in the standard manner.[15]

RESULTS

The hydrogen content of the a-Si_xH_y alloy films measured by the ^{15}N technique is given in Table I together with the dominant sample preparation conditions and the film microstructure, A, B, or C type. Irrespective of the other deposition parameters, samples prepared at low argon partial pressures ($\lesssim3\times10^{-3}$ Torr) exhibited a uniform smooth density with no structural features down to the 20 Å level (A-type microstructure). At higher argon partial pressures ($\gtrsim10\times10^{-3}$ Torr), low rf power ($\lesssim200$ W) and low (room-temperature) substrate temperatures, the deposited films exhibit a microstructure consisting of 50–200-Å high-density islands separated by a low-density network (B-type microstructure). At still higher argon partial pressures and/or higher rf power levels (>200 W) and/or higher substrate temperatures, the deposited films exhibit a two-level microstructure consisting of 300–500-Å-diam columns interspersed by a pronounced low-density network (C-type microstructure). These columns, in turn, are composed of 50–200 Å dimension high-density regions interspersed with

TABLE I. Typical sample preparation conditions, film structure, hydrogen content, and Si-2p binding energy.

Sample	Film structure	rf power (W)	Argon partial pressure ($\times10^{-3}$ Torr)	Hydrogen partial pressure ($\times10^{-3}$ Torr)	Substrate temperature (°C)	H/host (%)	Si-2p binding energy (eV)
132	A	400	1	1.7	RT[a]	40	99.2 ± 0.1
133	A	200	1	1.7	237	46	99.2 ± 0.1
134	A	400	1	1.7	233	...	99.2 ± 0.1
135	A	400	1	2×10^{-4}	RT	1	99.2 ± 0.1
150	A	425	1.0	0.1	RT	47	99.2 ± 0.1
151	A	425	1.0	9.2×10^{-2}	RT	55	99.2 ± 0.1
122	B	200	10	2×10^{-4}	RT	2	99.1 ± 0.1
125	B	100	10	1.7	RT	33	99.5 ± 0.1
141	B	200	10	1.7	241	26	99.3 ± 0.1
123	C	200	10	2×10^{-4}	225	2	99.0 ± 0.1
126	C	400	10	2×10^{-4}	RT	1	99.1 ± 0.1
142	C	200	10	1.7	325	25	99.4 ± 0.1
124	C	200	10	1.7	225	25	99.4 ± 0.1
98	C	400	10	1.7	RT	33	99.6 ± 0.1
119	C	200	10	1.7	RT	35	99.7 ± 0.1

[a] RT—room temperature.

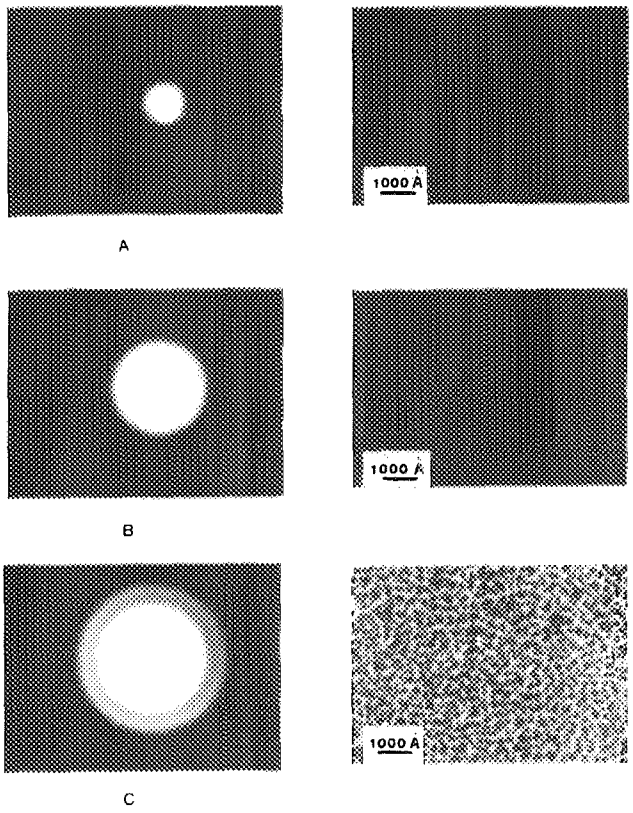

FIG. 1. Transmission electron micrographs and corresponding electron diffraction patterns of three a-Si_xH_y samples exhibiting A-, B-, and C-type microstructures.

low-density network regions. Transmission electron micrographs of three samples with A-, B-, and C-type microstructures and the corresponding electron diffraction patterns are shown in Fig. 1. All the samples examined are amorphous, as revealed by the halos in the diffraction patterns. It should be noted that all types of microstructures could be prepared independently of whether hydrogen was added or not. The addition of hydrogen appeared to give only second-order

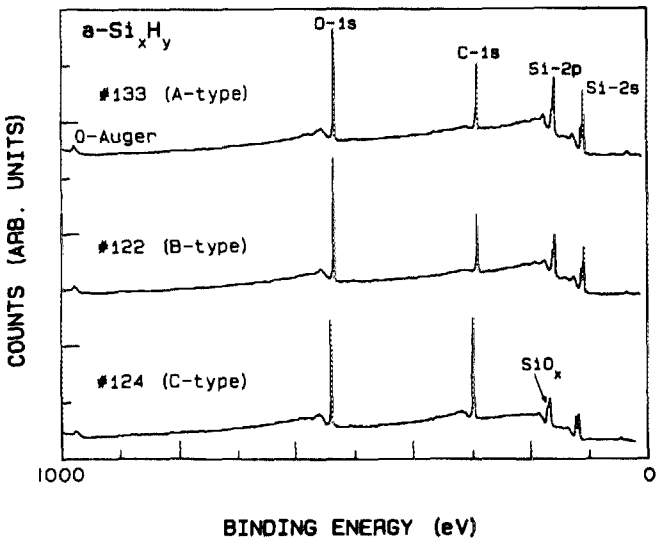

FIG. 2. Photoelectron spectra of three a-Si_xH_y samples with different microstructures: no. 133—A type, no.122—B type, and no. 124—C type.

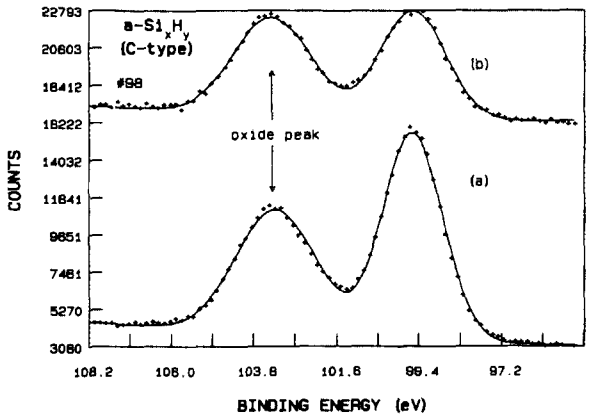

FIG. 3. Si-2p level spectra of sample no. 98 showing the effect of an HF etch on the oxide peak: (a) after etch and (b) before etch. The Si-2p binding energy remains unchanged.

effects on the microstructure, such as in increasing the total sputter pressure. However, the hydrogen partial pressure during deposition predominantly affects the hydrogen content in the films. Furthermore, the results from nuclear hydrogen profiling indicate that a-Si_xH_y films containing up to 50% hydrogen (H/host) can be prepared in all microstructure types by magnetron sputtering. Typically the films show a greater hydrogen concentration at the substrate-film interface and at the film surface.[15]

Typical XPS spectra in the binding energy range of 0–1000 eV for three different samples are shown in Fig. 2. All samples showed, other than carbon, the presence of oxygen, as evidenced from the O-1s line in these spectra. That some of the oxygen present is bonded to silicon in the form of silicon oxide is concluded from the presence of the Si-2p peak at ~ 104 eV. However, the presence of this oxide does not seem to affect the 2p binding energy of elemental silicon (bonded to hydrogen) which appears at ~ 98 eV. XPS analysis of samples subjected to an etching in 5% HF solution for 15 s[7] prior to mounting in the spectrometer showed that the Si-2p peak appearing at ~ 98 eV has the same binding energy before and after the etch even though the intensity of the oxide peak diminished as a result of etching (see Fig. 3). In both spectra shown in Fig. 3, the Si-2p peak due to silicon that is not bonded to oxygen occurs at 99.6 ± 0.1 eV.

A least-squares fitting of the Si-2p spectra from different samples to a Gaussian line shape showed a spread in Si-2p binding energy values between 99.1 and 99.7 eV (Table I). A cursory examination reveals that the binding energy does not seem to correlate with the hydrogen content in the samples. However, if the samples are grouped according to their microstructure (type A, B, or C), the outcome is remarkable. All samples with an A-type microstructure have a common Si-2p binding energy of 99.2 eV regardless of the hydrogen content in these samples. As an example, we show in Fig. 4 the Si-2p spectra from two samples both with type A microstructure but one with 1% H/host (sample no. 135) and the other with 40% H/host (sample no. 132). For both these samples the corrected Si-2p binding energy is 99.2 ± 0.1 eV. However, in samples with type B or type C microstructure, the Si-2p binding energy depends upon the

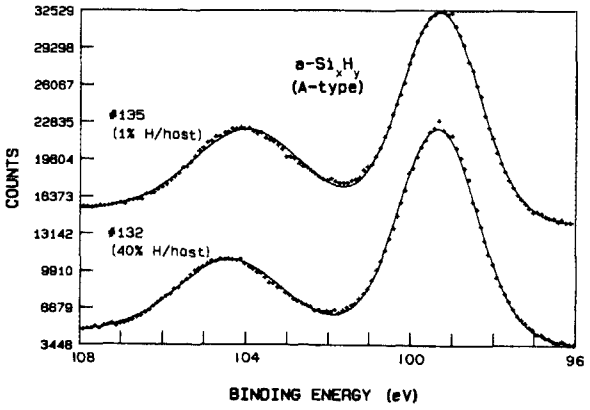

FIG. 4. Si-2*p* spectra of two samples both with A-type microstructure but different hydrogen content—sample no. 135 with 1% H/host and sample no. 132 with 40% H/host. Note that the binding energy is the same for the two samples.

hydrogen content (see Table I). In Fig. 5, we show the Si-2*p* spectra from three samples all with the same type of microstructure (type C) but with different hydrogen contents. As can be seen, the shift in the Si-2*p* line is largest for the sample with the highest hydrogen content. The Si-2*p* binding energy as a function of the hydrogen content for a *a*-Si$_x$H$_y$ samples with B-type and C-type microstructures is plotted in Fig. 6.

We note here that the oxide peak at ~ 104 eV exhibits a shift from sample to sample as seen in Figs. 4 and 5. However, the shift in the oxide peak position is not systematic and does not correlate with the shift in the Si-2*p* level. For example, in Fig. 4, whereas the Si-2*p* levels in samples nos. 135 and 132 exhibit no relative shift, the oxide peaks are shifted relative to each other. On the other hand, in Fig. 5, both the Si-2*p* levels and the oxide peaks in samples nos. 119 and 124 are shifted relative to the Si-2*p* level and the oxide peak position, respectively, in sample no. 123. Therefore, the oxide peak shift and the Si-2*p* level shift do not seem to share a common origin such as a Fermi-level shift in the sample. The oxide, it should be understood, is not well characterized and the oxide peak is probably an envelope of several oxides of variable stoichiometry SiO_x, with x varying from sample to sample.

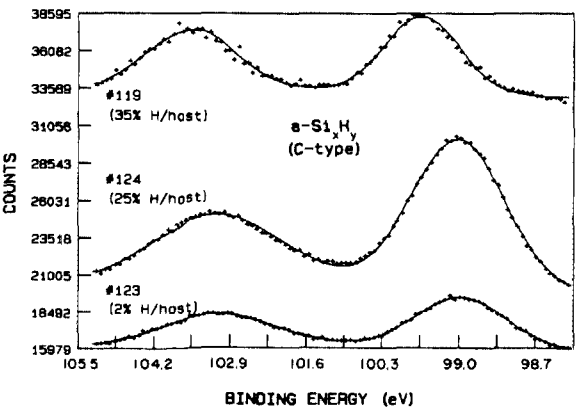

FIG. 5. Si-2*p* spectra of three samples with C-type microstructure. Sample no. 123 has 2% H/host, sample no. 124 has 25% H/host and sample no. 119 has 35% H/host. Note the shift in the binding energy with hydrogen content.

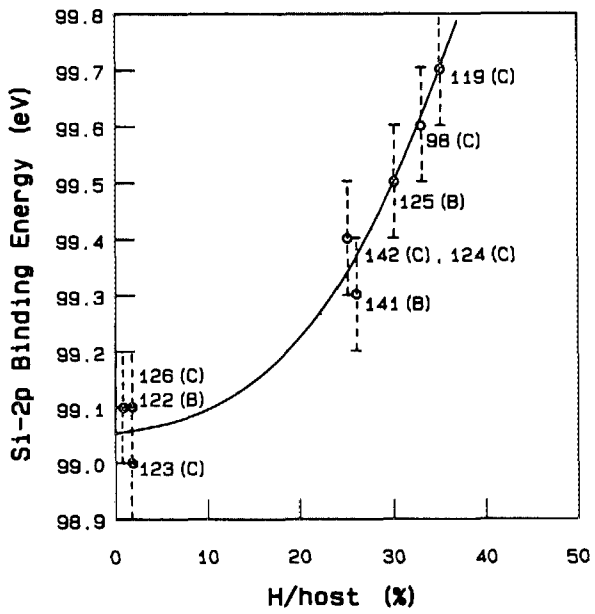

FIG. 6. The Si-2*p* binding energy plotted vs hydrogen content for several *a*-Si$_x$H$_y$ samples with B- and C-type microstructures.

We attribute the shift in the oxide peak to this variation in stoichiometry from sample to sample rather than to a shift in the Fermi level of the samples.

DISCUSSION

Usami *et al.*[7] have observed a shift of 0.15 eV in the Si-2*p* level due to hydrogenation in their sputtered *a*-Si:H films. However, they have not examined the microstructure of the hydrogenated films. Under similar preparation conditions as reported in their paper, we obtain films with A-type microstructure. To the extent that the precision of our XPS measurements is ± 0.1 eV, the results of Usami *et al.*[7] are similar to our results for A-type films. Gruntz *et al.*[9] have observed no chemical shift of the Si-2*p* level in amorphous hydrogenated silicon films prepared by sputtering. However, neither the microstructure of the films nor the preparation conditions are explicitly mentioned in their paper. The authors have, however, reported a chemical shift in the Si-2*p* line due to fluorination in dc sputtered amorphous fluorinated silicon films.[9] The authors obtain a main line at 99.6 ± 0.1-eV binding energy which they find is characteristic for pure silicon and with increasing fluorine content, the development of a satellite peak shifted by ~ 3.5 eV to higher binding energy. The intensity of the satellite peak is observed to scale with the fluorine content. Gruntz *et al.*[9] have fitted the Si-2*p* core level spectra of *a*-Si:F films under the following assumptions: (i) a total of five lines, corresponding to Si–Si_4, F–Si–Si_3, F_2–Si–Si_2, F_3–Si–Si, and SiF_4 configurations, contribute to each spectrum; (ii) the line shape is the same for each component; and (iii) the components are equally spaced. From analysis of several Si-2*p* spectra, the authors estimate an average chemical shift of 1.15 ± 0.02 eV per fluorine atom attached to a central Si atom. According to this model, therefore, for the same fluorine content, one would expect the smallest shift in the Si-2*p* level binding energy when all the fluorine is incorporated in the F–Si–Fi_3 configu-

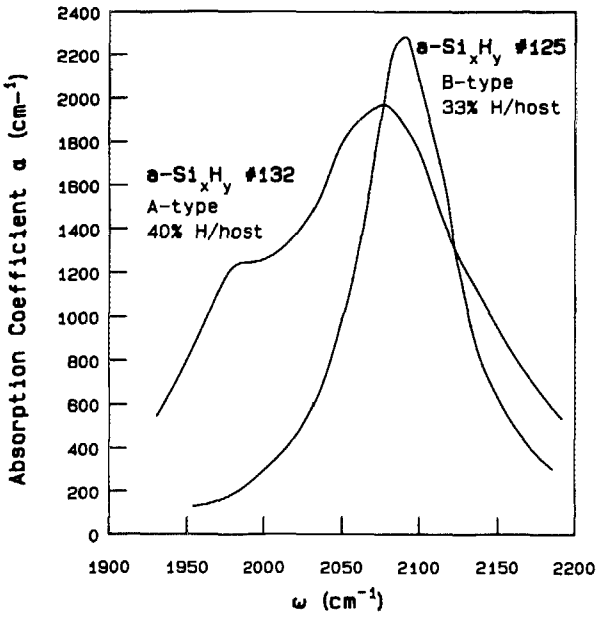

FIG. 7. Vibrational spectra of sample no. 132 (A-type microstructure) and sample no. 125 (B-type microstructure). Sample no. 132 has a hydrogen content of 40% H/host and sample no. 125 has a 33% H/host content.

ration and the largest shift when the fluorine is incorporated in the SiF_4 configuration. The intensity of the shifted satellite peak would, of course, scale with the fluorine content. Ley *et al.*[8] have analyzed high-resolution Si-2*p* core level spectra of hydrogenated amorphous silicon in a similar fashion and estimated a chemical shift of 0.335 ± 0.010 eV per hydrogen atom attached to the silicon atom.

The model of Gruntz *et al.*[9] provides a reasonable framework within which we can explain, qualitatively, our observation of the absence of any chemical shift in the Si-2*p* level binding energy in *a*-Si_xH_y films with A-type microstructure and a chemical shift scaling with hydrogen concentration in *a*-Si_xH_y films with type B and type C microstructures. We now propose that for any hydrogen content, *a*-Si_xH_y films with type A microstructure contain a proportionately larger fraction of the total hydrogen in the H–Si–Si_3 (monohydride) configuration compared to films with B-type or C-type microstructures which have proportionately a greater amount of the total hydrogen incorporated in the H_2–Si–Si_2 (dihydride) or H_3–Si–Si (trihidride) configurations. Since the expected chemical shift in the Si-2*p* binding energy is less for a single hydrogen atom attached to Si (i.e., for the H–Si–Si_3 configuration) than for two hydrogen atoms (i.e., the H_2–Si–Si_2 configuration) or for three hydrogen atoms (i.e., the H_3–Si–Si configuration) attached to a central Si atom, one would expect a smaller chemical shift in the Si-2*p* binding energy in *a*-Si_xH_y films with A-type microstructure and a much larger shift in films with B-type or C-type microstructures, for the same total hydrogen content. This explains why, within the precision limits of our XPS measurement and the accuracy of the Si-2*p* level curve fitting, we observe no shift in the Si-2*p* binding energy in films with A-type microstructure at any hydrogen content, whereas a shift is observed in films with B-type and C-type microstructures.

In confirmation of our hypothesis of different silicon-hydrogen bonding configurations in *a*-Si_xH_y films with dissimilar microstructures, we present the vibrational spectra in the frequency range 1900–2200 cm^{-1}, obtained by FTIR spectroscopy, for two *a*-Si_xH_y films (nos. 132 and 125) with similar hydrogen content, one with A-type microstructure and the other with B-type microstructure (Fig. 7). The spectra have been fitted with a combination of three Gaussian lines centered at 2000 cm^{-1} (corresponding to the SiH stretch mode), 2090 cm^{-1} (corresponding to the SiH_2 stretch mode), and 2150 cm^{-1} (corresponding to an environmentally different SiH stretch mode).[4] The strengths of the SiH, SiH_2, and the second SiH (denoted as SiH′) stretch modes in the two films are given in Table II. As tabulated, sample no. 132 with A-type microstructure contains proportionately more of the total hydrogen in the SiH (monohydride) configuration compared to sample no. 125 which exhibits a B-type microstructure.

Further confirmation of our hypothesis is provided by hydrogen evolution experiments reported previously.[15] The hydrogen evolution experiments in the range 300–1000 K show considerable structure. The films which have a C-type microstructure show occasionally a sharp peak in the rate of hydrogen evolution at ~200 °C and always show a large evolution broad maximum at ~450 °C, with perhaps a shoulder at ~630 °C. Hydrogen is evolved at all temperatures, however, with the evolution starting at ~100 °C. Films with a B-type microstructure show a similar hydrogen evolution rate temperature dependence, though often the low-temperature peak is sharper and the shoulder more pronounced. A-type structure films have a different hydrogen evolution pattern, showing two distinct maxima at approximately 370 and 410 °C and a high-temperature maximum at 610 °C. The hydrogen evolved at low temperatures (~375 °C) has been tentatively assigned to the escape of hydrogen from SiH_2 or SiH_3 bonds in the low-density network in the films,[18] whereas hydrogen evolved at 600 °C and above is associated with the breaking of isolated SiH bonds. To investigate the relative differences between the

TABLE II. Relative strengths *C* of the SiH ($\omega = 2000\,cm^{-1}$), SiH_2 ($\omega = 2090\,cm^{-1}$), and SiH′ ($\omega = 2150\,cm^{-1}$) stretch modes in *a*-Si_xH_y samples no. 132 and no. 125.

Sample	Film structure	H/host (%)	$\frac{C_{SiH}}{C_{SiH}+C_{SiH_2}+C_{SiH'}}$	$\frac{C_{SiH_2}}{C_{SiH}+C_{SiH_2}+C_{SiH'}}$	$\frac{C_{SiH'}}{C_{SiH}+C_{SiH_2}+C_{SiH'}}$
132	A	40	0.26	0.41	0.33
125	B	33	...	1.0	...

low-temperature behavior for different film microstructures, known volumes of samples with predetermined hydrogen content (measured by nuclear ^{15}N technique) and microstructure were cycled through a linear temperature ramp up to 600 °C with the evolved hydrogen being measured continuously. The results of such evolution experiments show that for the same total hydrogen content, the C-type microstructure always contains more weakly bonded hydrogen than B or A. This result implies that SiH_2 and SiH_3 bonding configurations occur in both featureless and columnar structures, but more of the SiH bonding occurs in the featureless microstructure, i.e., A-type microstructure.

The scaling of the shift in the Si-2*p* binding energy with hydrogen content in films with B-type and C-type microstructures may be explained by one or a combination of two effects: (i) shift in the Fermi level and (ii) increase in the proportion of SiH_2 and/or SiH_3 bonding configurations at higher hydrogen concentrations. We know from measurements of optical gap and electrical activation energy in these films that the Fermi level can vary by several tenths of an electron volt from one film to another depending on the preparation conditions, the hydrogen content, and the microstructure. However, hydrogen evolution studies also indicate that at higher levels of hydrogen content, a-Si_xH_y films, for all types of microstructures, contain larger fractions of the total incorporated hydrogen in SiH_2 and/or SiH_3 configurations.[15] To resolve quantitatively the relative contributions of the two effects in the scaling of the Si-2p level shift with hydrogen content would require a more sophisticated fit to our XPS data (in the manner of Gruntz *et al.*[9]) by at least four lines, corresponding to Si–Si_4, H–Si–Si_3, H_2–Si–Si_2, and H_3Si–Si configurations using known strengths calculated from vibrational data, instead of the single Gaussian line shape employed in the present study. Such an effort is currently being undertaken and the results will be presented later.

CONCLUSIONS

Amorphous Si_xH_y alloy films prepared by planar, reactive, rf magnetron sputtering exhibit three distinct types of microstructures depending on the deposition conditions: (i) type A with no discernible microstructural features down to the 20-Å level and with a smooth uniform density; (ii) type B consisting of high-density regions of 50–200-Å lateral dimensions separated by a low-density network; and (iii) a two-level (type C) microstructure consisting of 300–500-Å dimension columns separated by a pronounced low-density network. The columns, in turn, are composed of 50–200-Å dimension high-density regions interspersed with low-density network.

The Si-2*p* level, measured by x-ray photoelectron spectroscopy using Al $K\alpha$ excitation, shows no chemical shift in a-Si_xH_y films with A-type microstructure, regardless of the hydrogen content. However, in a-Si_xH_y films with B-type and C-type microstructures, a chemical shift is observed in the Si-2*p* level which scales with the hydrogen content of the film.

The difference in the Si-2*p* level photoelectron spectra of A-type films and B- and C-type a-Si_xH_y films are explained in terms of the differences in the silicon-hydrogen bonding configurations. Data from Fourier-transform infrared and hydrogen evolution experiments are presented in support of the model.

[1]See, for example, *Amorphous Semiconductors*, edited by M. H. Brodsky (Topics in Applied Physics, Vol. 36) (Springer, Heidelberg, 1979).
[2]See, for example, *Hydrogenated Amorphous Silicon*, edited by J. I. Pankove (Semiconductors and Semimetals, Vol. 21) (Academic, Orlando, FL, 1984).
[3]M. H. Brodsky, M. Cardona, and J. J. Cuomo, Phys. Rev. B **16**, 3556 (1977).
[4]E. C. Freeman and W. Paul, Phys. Rev. B **18**, 4288 (1978).
[5]J. C. Knights, G. Lucovsky, and R. J. Nemanich, Philos. Mag. B **37**, 467 (1978).
[6]C. J. Fang, L. Ley, H. R. Shanks, K. J. Gruntz, and M. Cardona, Phys. Rev. B **22**, 6140 (1980).
[7]K. Usami, T. Shimada, and Y. Katayama, Jpn. J. Appl. Phys. **19**, L389 (1980).
[8]L. Ley, J. Reichart, and R. L. Johnson, Phys. Rev. Lett. **49**, 1664 (1982).
[9]K. J. Gruntz, L. Ley, and R. L. Johnson, Phys. Rev. B **24**, 2069 (1981).
[10]G. A. N. Connell and J. R. Pawlik, Phys. Rev. B **13**, 787 (1976).
[11]H. Wagner and W. Beyer, Solid State Commun. **48**, 585 (1983).
[12]J. B. Webb, J. Appl. Phys. **53**, 9043 (1982).
[13]J. B. Webb and S. R. Das, J. Appl. Phys. **54**, 3282 (1983).
[14]S. R. Das, D. F. Williams, and J. B. Webb, J. Appl. Phys. **54**, 3101 (1983).
[15]S. R. Das, R. Charbonneau, D. F. Williams, J. B. Webb, J. R. MacDonald, D. R. Polk, S. Zukotynski, and J. Perz, Can. J. Phys. **63**, 852 (1985).
[16]Y. Z. Sun, S. R. Das, D. F. Williams, and J. B. Webb, J. Appl. Phys. **59**, 3160 (1986).
[17]J. A. Dobrowolski, F. C. Ho, and A. Waldorf, Appl. Opt. **22**, 3191 (1983).
[18]R. A. Street, J. C. Knights, and D. K. Biegelsen, Phys. Rev. B **18**, 1880 (1978).